Fatigue Crack Growth Rate, Crack Paths and Microstructure Changes in TRIP Steel

Michael Janssen[1] and Xu Cheng[2]

[1] Department of Material Science and Engineering, Delft University of Technology, Mekelweg 2, 2628 CD, Delft, The Netherlands (M.Janssen@tudelft.nl)
[2] Netherlands Institute *for* Metals Research, Mekelweg 2, 2628 CD, Delft, The Netherlands (X.Cheng@nimr.nl)

ABSTRACT. *Load-controlled fatigue tests were conducted for four positive R values on a low-alloy TRIP steel for two different heat treatments: an optimal treatment leading to retained austenite (next to ferrite, bainite and martensite) and a non-optimal treatment leading to a ferritic-martensitic steel. A significantly increased resistance to fatigue crack growth was found for the optimal case relative to the non-optimal case. The amount of crack closure was found to be larger in case of the non-optimally treated (ferritic-martensitic) steel. Martensite transformation, as was observed on the basis of an increasing hardness during straining in static tensile tests, was only found to occur within the monotonic plastic zone formed during fatigue.*

INTRODUCTION

Transformation-Induced Plasticity (TRIP) steels are used for safety-based car bodies, because of the high energy absorption potential under dynamic loading as occurs during car crashes [1]. Furthermore, the usage of TRIP steels is thought to extend to cyclically loaded wheel rim, suspension and door hinges etc., where currently ferritic-martensitic steels are used [2]. Therefore, there is a need to also understand the fatigue behaviour of TRIP steels. Until now only little research is performed on the fatigue behaviour of TRIP steels. This research indicates that TRIP steels exhibit cyclic hardening, which is mainly associated with the development of internal stresses [2, 3]. However, the research on fatigue crack growth behaviour of TRIP steels is still very limited. In the present study, the main object is to observe the fatigue crack growth, crack path and microstructure changes under fatigue loading with different (positive) *R* values in a low-alloy TRIP steel.

MATERIAL AND EXPERIMENTAL PROCEDURES

The material used in this study is a cold-rolled (1.8 mm thick) low-alloy TRIP steel. Table 1 gives the chemical composition. Here Si, Al and P play a key role in the TRIP-effect, because they inhibit cementite formation during the bainitic transformation.

Table 1. Chemical composition of the TRIP steel (wt. %)

C	Mn	Si	Al	P
0.188	1.502	0.254	0.443	0.015

Initially all test specimens were annealed at 600 °C for 24 hours and cooled down slowly in order to reduce residual stresses as much as possible.

On a number of specimens a heat treatment was carried out at an intercritical annealing temperature of 800 °C for 30 minutes, creating a microstructure of ferrite and austenite. This was followed by fast cooling to the bainite formation temperature regime (400 °C) and holding this temperature for 1 minute during which a certain amount of bainite is formed. Finally, the material was quenched to room temperature after which the least stable austenite transforms into martensite. In the resulting material, the microstructure consists of ferrite, bainite, retained austenite and a little martensite. The volume fraction of retained austenite is 4.9 %, which was measured from X-ray. This heat treatment is designated as "optimal".

In order to assess the influence of the TRIP effect, a heat treatment was carried out on the remaining specimens without the procedure of holding at the bainite transformation temperature, which leads to a ferritic-martensitic steel containing only very small amounts of retained austenite and bainite. The volume fraction of martensite is about 50 %, calculated from the pseudo binary phase diagram using Thermocalc software (KTH-Sweden). In contrast with the optimal heat treatment, this treatment will be designated as "non optimal".

Standard sheet-shaped tensile specimens according to ASTM E8M, with a gauge length of 32mm and a width of 6mm, were used for static tensile tests to measure the mechanical properties of the material after the optimal and the non-optimal heat treatments. These tests were carried out on an INSTRON 5500R-4505 testing machine (100 kN load capacity). The measured mechanical properties are shown in Table 2.

Table 2. Mechanical properties of the TRIP steel

Heat treatment	Yield strength (MPa)	Tensile strength (MPa)	Strain at fracture (%)
Non optimal	667	1379	13.2
Optimal	430	921	22.3

Load-controlled fatigue tests were performed at room temperature on centre-notched specimens, using a servo-hydraulic test machine (MTS810, 100 kN load capacity). Cyclic tension was applied to the specimens at a frequency of 10Hz. Four R values ($R = \sigma_{min}/\sigma_{max}$), 0.1, 0.3, 0.5 and 0.7 were employed, using the same maximum stress for all

tests (σ_{max} = 142 MPa). The specimens were prepared according to ASTM standard ASTM E647, as shown in Figure 1.

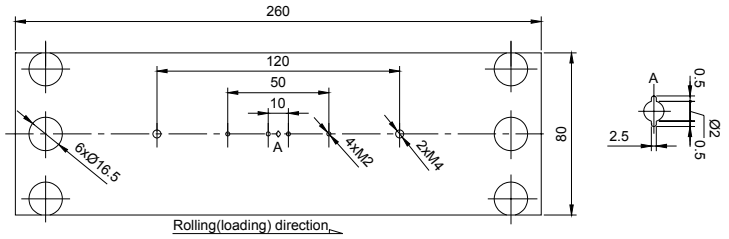

Figure 1. Geometry of fatigue specimens according to ASTM standard ASTM E647.

Development of the failure crack was monitored by using a four-wire pulsed potential-drop method during the fatigue tests. After failure, the fracture surfaces were observed using an SEM. Furthermore, cross sections of the crack on planes parallel to the loading direction and perpendicular to the surface were observed to characterise the crack path and possible transformation of retained austenite to martensite due to the TRIP effect. Additionally, a micro-Vickers hardness tester was used to measure the hardness along the crack on the plate surface at different distances from the crack plane.

EXPERIMENTAL RESULTS AND DISCUSSION

Deformation behaviour

In order to demonstrate the TRIP effect in the present material, the engineering stress-strain curves for the non-optimal and optimal heat-treatment conditions are shown in Figure 2(a). Clearly, the material after the non-optimal heat-treatment has a higher tensile strength and a smaller strain at fracture compared to the optimal heat-treatment condition.

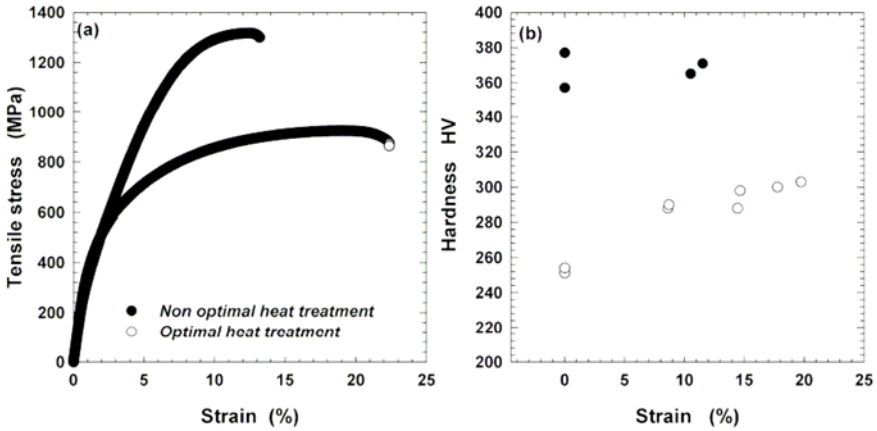

Figure 2. Deformation behaviour after non-optimal and optimal heat treatment: (a) engineering stress-strain curve and (b) development of Vickers hardness with strain.

Additionally, Vickers hardness tests were carried out in the uniformly deformed area of the specimen at regular strain intervals during the static tensile tests, as shown in Figure 2(b). The Vickers hardness in the material with the non-optimal heat treatment remained at a constant level (370 ± 10 HV), while that of the optimally heat-treated material increased significantly with increasing strain. It can be expected that during plastic straining retained austenite will transform into martensite. It is known that the resulting intense local plastification enforces a strong hardening and consequently a significant increase of uniform strain [4,5]. In the present material in the optimal heat treatment condition, the hardness increases approximately 20% compared to the original material, indicating that transformation of retained austenite occurs during straining.

Fatigue crack growth rate

In the present work, fatigue tests were carried at a constant frequency (10Hz) and a constant maximum stress, using four *R*-ratio values. Figure 3 shows the crack growth rates after both heat treatments. A significant increase in resistance to fatigue crack growth can be observed in the optimally heat-treated material. This might be due to the presence of retained austenite, an aspect that will be discussed below.

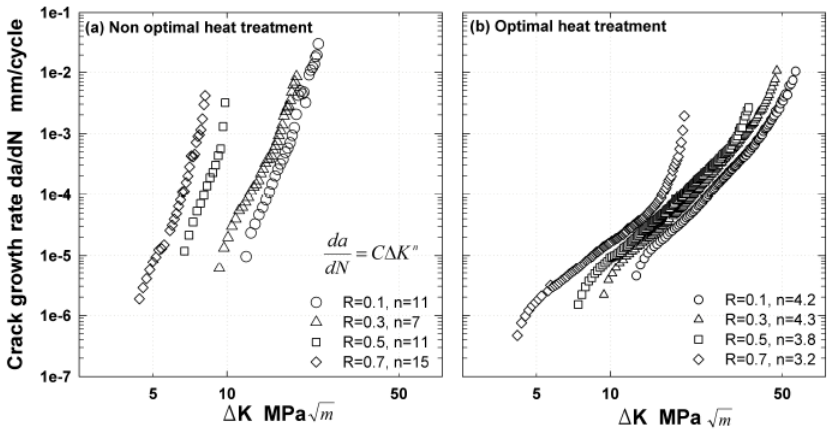

Figure 3. Fatigue crack growth rates at σ_{max} = 142 MPa: (a) after non-optimal heat treatment and (b) after optimal heat treatment.

The crack growth rates are generally higher in the non-optimally heat treated material (Figure 3(a)), especially at higher ΔK values. Also the slopes of the crack growth curves, signified by the exponent in the Paris equation $da/dN = C(\Delta K)^n$, are higher (n = 7 ~ 15) than in optimally heat-treated material (n = 3.2 ~ 4.3). The steel after a non-optimal heat treatment predominantly consists of a ferrite-martensite dual phase microstructure. It is known that for low cycle fatigue in ferritic-martensitic steels, due to the large amount of interfacial area between ferrite and martensite, a low strain amplitude already provides many crack initiation sites [6]. This possibly is the reason for the larger dependence of the crack growth rate on ΔK for the non-optimally heat-treated steel, as expressed by the higher n values.

It is generally assumed that in TRIP steel strain-induced martensite formation in the crack tip plastic zone increases the amount of crack closure and that this is the reason

for the lower fatigue crack growth rate [7]. However, from figure 3 it can be seen that the R ratio has more effect in the non-optimally treated steel, suggesting a larger amount of crack closure. This aspect will be further discussed below.

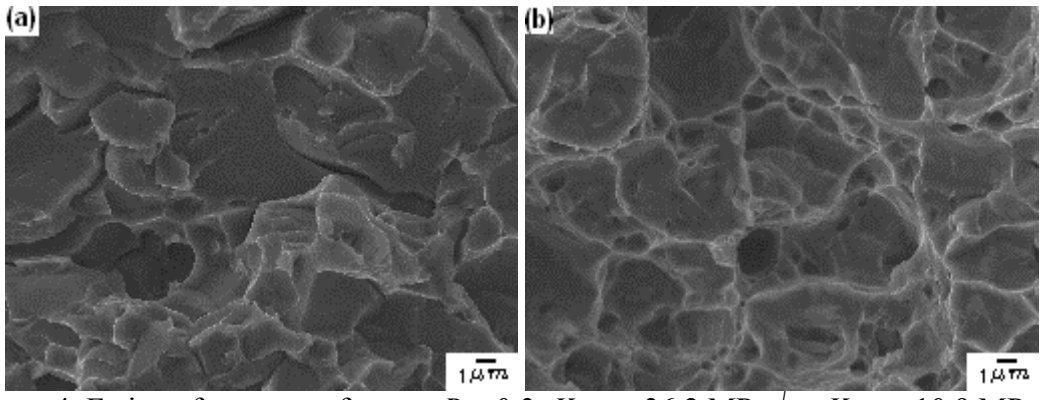

Figure 4. Fatigue fracture surfaces at R = 0.3, K_{max} = 36.2 MPa√m, K_{min} = 10.9 MPa√m of (a) non-optimally heat-treated and (b) optimally heat-treat TRIP steel.

Fractography

Two SEM micrographs of the fatigue fracture surface of non-optimally and optimally heat treated material are shown in Figure 4. Figure 4(a) reveals a quasi-cleavage-like fracture surface, on which only limited plastic deformation can be observed. This brittle fracture is consistent with the higher crack growth rate found. Figure 4(b) reveals a dimpled fracture surface resulting from void nucleation, growth and coalescence, indicating that a large amount of plasticity is involved. It might be assumed that a larger amount of plastic deformation, as occurs in optimally heat-treated material, causes more energy to be absorbed as a result of which fatigue crack growth is reduced [7].

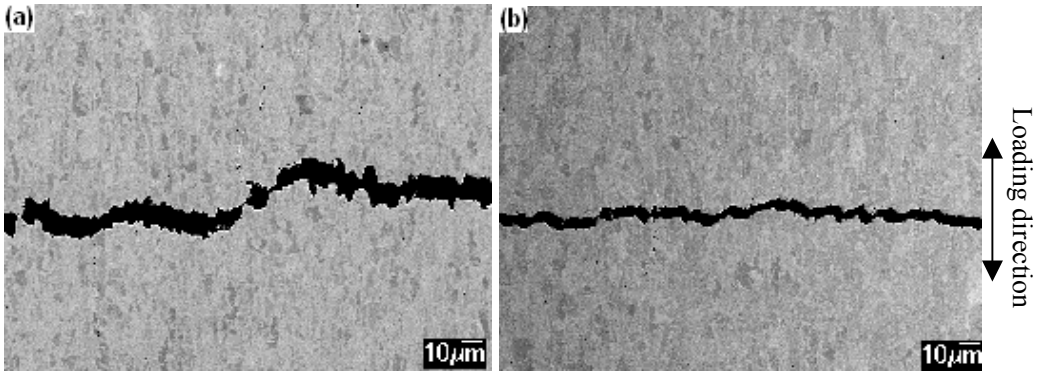

Figure 5. Cross sections perpendicular to the plate surface of cracks grown at R = 0.1 for (a) non-optimal heat treatment and (b) optimal heat treatment.

Figure 5 shows cross sections of the crack taken perpendicular to the plate surface at 9 mm from the specimen centre for both heat treatment conditions tested at R = 0.1. The two samples were taken from the fatigue specimens in the unloaded state when the cracks had reached a half length of 11.3 mm (in Figure 5(a)) and 11.9 mm (in Figure 5(b)) respectively. Comparing these figures, a larger crack opening can be observed in

the case of non-optimally heat-treated steel, which seems to be caused by surface-induced closure. More closure is consistent with the observation made earlier on the basis of the measured crack growth rates (see previous section). Apparently, crack closure cannot be the explanation for the lower crack growth rate of optimally treated steel. At present we do not yet have an alternative explanation available.

Martensitic transformation

Following Irwin, the half monotonic plastic zone size as a result of the maximum fatigue load can be estimated by the following equation:

$$r_p = \frac{1}{2\pi}\left(\frac{K_{\max}}{\sigma_{ys}}\right)^2 \tag{1}$$

where K_{max} is the maximum mode I stress intensity factory and σ_{ys} is the yield strength. In the present fatigue tests, the maximum load was constant (σ_{max} = 142 MPa), while different R values were used. Consequently, the change of the monotonic plastic zone size only depends on the fatigue crack length.

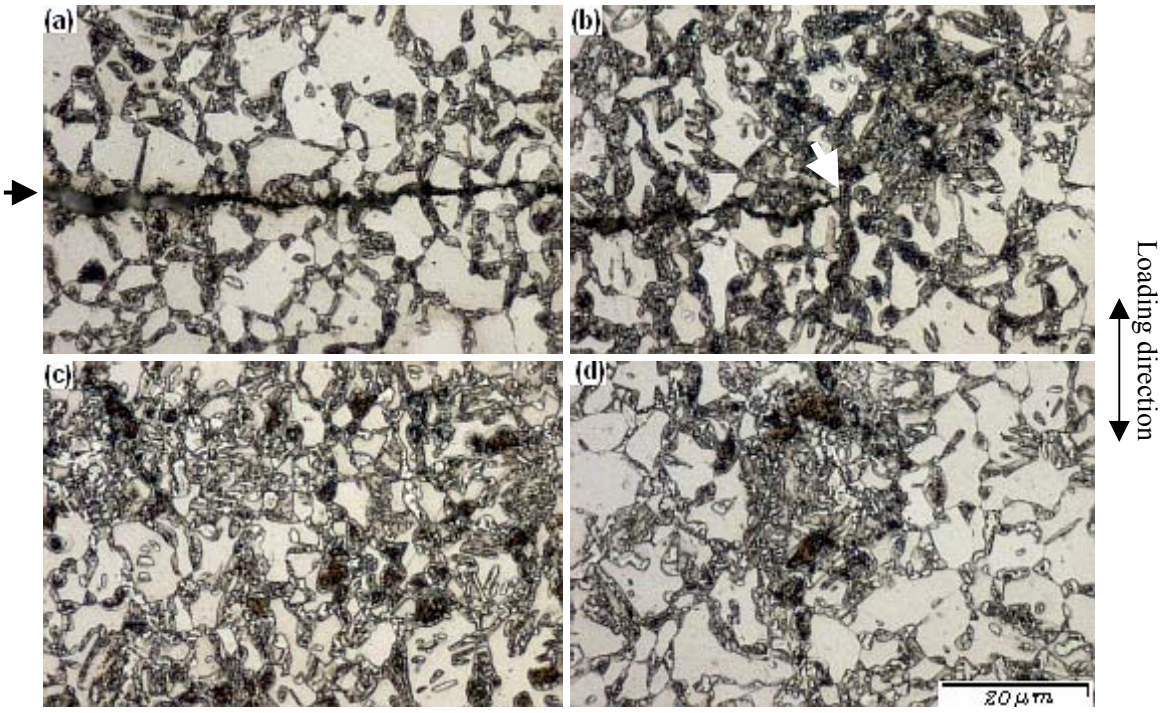

Figure 6. Optical micrographs at or close to a crack grown at R = 0.1, σ_{max} = 142 MPa (arrows indicate crack and crack tip): (a) half crack length a = 3.5 mm, (b) at crack tip (a = 10 mm), (c) 5 mm from the crack plane at *(a)* position, (d) 5 mm from the crack plane at *(b)* position.

Figure 6 shows the microstructure after the optimal heat treatment close to and at some distance from fatigue cracks grown at R = 0.1. Etching was performed in a 10 g/liter solution of metabisulphite for 20 seconds, followed by 4% picral acid for 60

seconds. This leads to ferrite in grey, austenite in white and bainite and martensite in dark-brown. Figures 6(a) and 6(b) show the microstructure at a half crack length of 3.5 mm (K_{max} = 15.0 MPa√m) and at the tip where the half crack length is 10 mm (K_{max} = 26.2 MPa√m) respectively. The monotonic plastic zone sizes are 0.19 and 0.59 mm respectively. Close to the crack flanks (Figures 6(a) and (b)), *i.e.* inside the monotonic plastic zone, a relatively large amount of dark-brown phases can be observed. However, 5 mm from the crack plane, *i.e.* outside the monotonic plastic zone, much more white phase can be found, indicating that more retained austenite is still present there (Figure 6(c) and (d)). In TRIP steel bainite is assumed to be a stable phase during mechanical loading, *i.e.* it is not formed and does not transform. Therefore, in Figures 6(a) and (b), the large quantities of the dark phase indicate that retained austenite is transformed into martensite along the crack flanks. A similar result is reported from recent research on high strength steel [7].

Vickers hardness measurements were carried out on the plate surface along lines parallel to the crack at 0.25 mm and 5.25 mm distance. A load of 1 kg was used to ensure an indentation size that is large enough relative to the microstructure. Figure 7 shows the results for both heat treatment conditions. In non-optimally heat-treated material (see Figure 7(a)), the average Vickers hardness was 373 HV at 0.25 mm and 375 HV at 5.25 mm distance from the crack. This indicates that the hardness is not affected by the presence of the crack. In optimally heat-treated material (see Figure 7(b)), the average hardness outside the monotonic plastic zone (○ mark, 5.25 mm line) is 243 HV, while inside (● mark, 0.25 mm line) this is 258 HV, an increase of approximately 6 %. This same tendency was also observed for R = 0.3, 0.5 and 0.7. In TRIP-assisted multiphase steels, it is observed that ferrite is the softest phase, followed by bainite, austenite and martensite [8]. Therefore, an increase of the hardness can probably be attributed to the transformation of retained austenite into martensite. Note that the scatter in the hardness values is thought to be due to the non-homogeneity of the material itself.

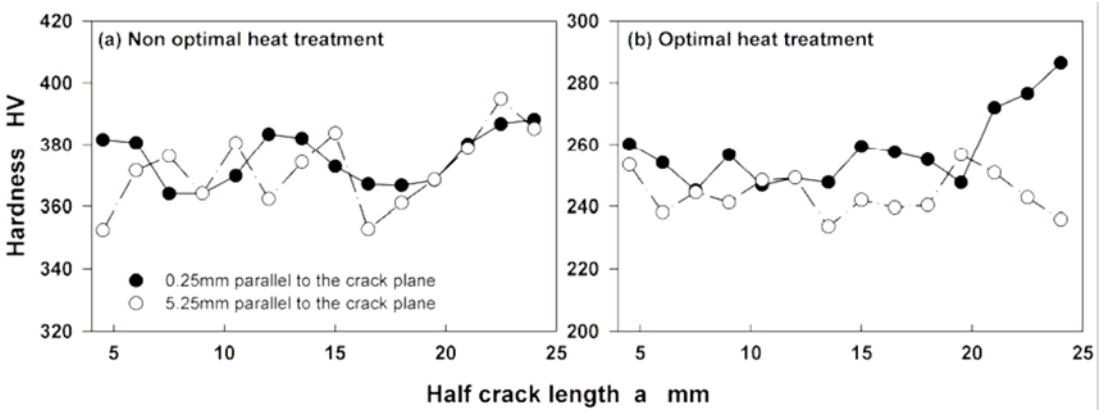

Figure 7. Hardness variation parallel to the plane of a crack grown at R = 0.1, σ_{max} = 142 MPa, (a) non-optimal heat treatment and (b) optimal heat treatment.

CONCLUSIONS

Fatigue tests were performed for four R values on cold-rolled low-alloy TRIP steel that was heat treated to contain a maximum amount of retained austenite and to a predominantly ferritic-martensitic structure respectively.

- The two different heat treatments affected the mechanical properties remarkably.
- Only in optimally heat-treated steel, the hardness increased with increasing strain during static tensile tests.
- A significantly higher resistance to fatigue crack growth is found in case of steel containing retained austenite.
- The crack growth rate in non-optimally heat-treated material (*i.e.* ferritic-martensitic steel) increases rapidly with ΔK.
- In TRIP steel containing retained austenite less crack closure occurs compared to the ferritic-martensitic variant.
- Transformation of retained austenite into martensite was only observed inside the monotonic plastic zone formed by fatigue crack growth. The Vickers hardness inside the monotonic plastic zone was higher than that outside.

ACKNOWLEDGEMENTS

The authors are grateful to NIMR (Netherlands Institute *for* Metals Research) for their financial support of this work through the project "Fatigue crack initiation and propagation in DP and TRIP steels".

REFERENCES

1. B.C. De Cooman, Structure-properties relationship in TRIP steels containing carbide-free bainite, *Solid State & Materials Science*, **8**, (2004), 285-303.
2. Shin-ichi Yasuki, Low Cycle Fatigue-Hardening of TRIP-Aided Dual-Phase Steels, *J. Japan Inst. Metals*, **Vol. 54**, No.12 (1990), 1350-1357.
3. Koh-ichi Sugimoto, Effect of Prestraining on Low Cycle Fatigue Properties of Low Alloy TRIP Steels, *J. Soc. Mat. Sci., Japan*, **Vol. 50**, No.6 (June 2001), 657-664.
4. F.D. Fischer, G. Reisner, E. Werner, K. Tanake, G. Cailletaud, T. Antretter, A new view on transformation induced plasticity (TRIP), *International Journal of Plasticity*, **16** (2000), 723-748.
5. P.J. Jacques, Transformation-induced plasticity in steels, Thermodynamics, Microstructures and Plasticity, 2003, 241-250
6. P.C. Chakraborti, M.K.Mitra, Room temperature low cycle fatigue behaviour of two high strength lamellar duplex ferrite-martensite (DFM) steels, *International Journal of Fatigue,* **27** (2005) 511-518.
7. C.Y. Huo and H.L. Gao, Strain-induced martensite transformation in fatigue crack tip zone for a high strength steel, *Materials Characterization*, **55** (2005), 12-18
8. Q. Furnémont, M. Kempf, P.J. Jaques, M. Göken and F. Dlannay, On the measurement of the nanohardness of the constitutive phase of TRIP-assisted multiphase steels, *Materials Science and Engineering*, **A328** (2002) 26-32.